Environ. Sci. Technol. 1999, 33, 3653–3660

Coupling of Phytoplankton Uptake and Air–Water Exchange of Persistent Organic Pollutants

JORDI DACHS,† STEVEN J. EISENREICH,*,† JOEL E. BAKER,‡ FUNG-CHI KO,‡ AND JEFF D. JEREMIASON†

Department of Environmental Sciences, Rutgers University, 14 College Farm Road, New Brunswick, New Jersey 08901-8551, and Chesapeake Biological Laboratory, University of Maryland, P.O. Box 38, Solomons, Maryland 20688

A dynamic model that couples air–water exchange and phytoplankton uptake of persistent organic pollutants has been developed and then applied to PCB data from a small experimental lake. A sensitivity analysis of the model, taking into account the influence of physical environmental conditions such as temperature, wind speed, and mixing depth as well as plankton-related parameters such as biomass and growth rate was carried out for a number of PCBs with different physical–chemical properties. The results indicate that air–water exchange dynamics are influenced not only by physical parameters but also by phytoplankton biomass and growth rate. New phytoplankton production results in substantially longer times to reach equilibrium. Phytoplankton uptake-induced depletion of the dissolved phase concentration maintains air and water phases out of equilibrium. Furthermore, PCBs in phytoplankton also take longer times to reach equilibrium with the dissolved water phase when the latter is supported by diffusive air–water exchange. However, both model analysis and model application to the Experimental Lakes Area of northwestern Ontario (Canada) suggest that the gas phase supports the concentrations of persistent organic pollutants, such as PCBs, in atmospherically driven aquatic environments.

Introduction

Air–water exchange and phytoplankton uptake are two of the most relevant processes affecting the fate of persistent organic pollutants (POPs) in aquatic environments (*1–3*). Phytoplankton uptake is the first step in the bioaccumulation of POPs in aquatic food webs, and air–water exchange is one of the main pathways for entry and loss (*4, 5*). Phytoplankton also play a major role in the occurrence and biogeochemical cycles of these pollutants in the oceans. POPs uptake by phytoplankton and their removal from surface waters by settling of large particles explains observed vertical profiles in the water column (*6–13*). Furthermore, there are potential interactions between trophic status (e.g., biomass and growth rate dilution) and the occurrence and cycling of POPs (*14*). Higher biomass results in lower concentrations of POPs in phytoplankton (*15, 16*) and high phytoplankton growth may also lead to a significant dilution of the POP concentrations (*17, 18*). Increased vertical fluxes in the water column and higher PCB concentrations in benthic organisms due to eutrophication have been observed (*9, 19, 20*). However, the interactions between bioaccumulation dynamics and air–water exchange have not been studied even though there are a number of observations that suggest that air–water exchange and phytoplankton uptake are coupled. Profiles of PAH and PCB concentrations observed in the dissolved and particulate phase of the water column are frequently similar to those found in the gas phase (*2, 19*). Furthermore, the occurrence of POPs in aquatic food webs in pristine environments suggests an air–water–phytoplankton process (*4*).

The objectives of the present paper are to study the mutual influences between air–water and water–phytoplankton exchange processes and to determine whether air–water exchange can support POP concentrations observed in aquatic environments. To accomplish this a model for air–water–phytoplankton exchange will be developed, allowing the linkages between air–water exchange and phytoplankton uptake to be elucidated. The model will then be applied to real limnetic ecosystems from the Experimental Lakes Area in Canada.

Model Description

Phytoplankton Uptake and Air–Water Exchange. To compare air–water with water–phytoplankton exchange, the equations describing both processes are examined. Phytoplankton uptake of POPs may be described as (*21–23*)

$$\frac{dC_P}{dt} = k_u C_W - k_d C_P - k_G C_P \qquad (1)$$

where C_P (ng kg^{-1}) and C_W (ng m^{-3}) are the POP concentrations in phytoplankton and water, respectively, and k_u (m^3 kg^{-1} d^{-1}) and k_d (d^{-1}) are uptake and depuration constants, respectively. k_G (d^{-1}) is the growth rate of the phytoplankton community or biomass (*22*). For a self-sustained biomass, k_G will have a value of zero, while for a phytoplankton community that doubles its biomass in one day, it will have a value of one. Equation 1 describes a one-compartment model, but there is strong evidence from experimental work that uptake is best fit with a two-compartment model, which is described by a second set of uptake and depuration constants (*23*). In practice, the uptake from water into one of the compartments is sufficiently fast that it is assumed to be in equilibrium with the water phase. This is usually identified as surface adsorption or partitioning into the cell membrane (*23, 24*). For the second compartment, the concentration is obtained by integrating eq 1 assuming a constant water concentration. Therefore, the POP concentration in phytoplankton is described by

$$C_P(t) = K_{SA} C_W + C_{P,eq}(1 - e^{-(k_d + k_G)t}) \qquad (2)$$

where K_{SA} (m^3 kg^{-1}) is the surface sorption coefficient and $C_{P,eq}$ (ng/g) is the concentration in the phytoplankton matrix in equilibrium with the water phase. Laboratory experiments of POP uptake by phytoplankton are usually carried out beginning with zero concentration in the phytoplankton and near constant concentrations in the water. In these experiments, the fast first step in the uptake dynamics is used to estimate K_{SA}, while the exponential approach to equilibrium

* Corresponding author phone: (732)932-9588; fax: (732)932-3562; e-mail: eisenreich@envsci.rutgers.edu.
† Rutgers University.
‡ University of Maryland.

10.1021/es990168o CCC: $18.00
Published on Web 09/14/1999

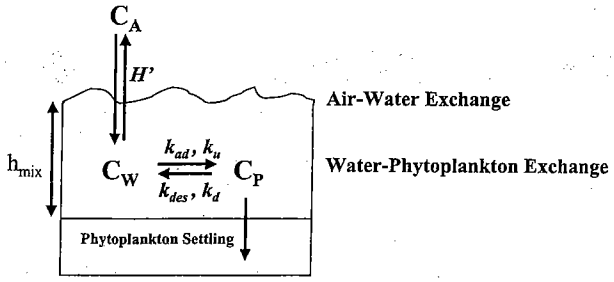

FIGURE 1. Schematic of the air–water–phytoplankton exchange process. C_A, C_W, and C_P are the POP concentrations in the gas phase, water, and phytoplankton, respectively; h_{mix} is the mixing depth of the water column; k_{ad} and k_u are the uptake constants; and k_{des} and k_d are the depuration constants. See text for full explanations.

is fitted using eq 2 to obtain estimations of $C_{P,eq}$ and K_d (*25*). Finally, uptake constants are obtained considering the equilibrium conditions:

$$k_u = \frac{C_{P,eq}}{C_W}(k_d + k_G) \tag{3}$$

where the values of k_{SA}, k_u, and k_d obtained are dependent on the chemical–physical properties of the POP and the phytoplankton species (*23, 25*).

The air–water exchange flux may be obatained by applying the traditional two-layer model (*5, 26–28*):

$$F_{A-W} = k_{ol}\left(C_W - \frac{C_A}{H'}\right) \tag{4}$$

$$\frac{1}{k_{ol}} = \frac{1}{k_W} + \frac{1}{k_A H'} \tag{5}$$

where C_A is the POP concentration in air (ng m^{-3}), H' is the dimensionless Henry's law constant corrected for temperature, k_{ol} (m d^{-1}) is the overall mass-transfer rate between air and water, and k_W (m d^{-1}) and k_A (m d^{-1}) are the water-side and air-side transfer rates, respectively. Details on methods and correlations used for estimation of H' and k_{ol} can be found in the above references.

Water–Phytoplankton Fluxes for Constant Water Concentration. When the POPconcentration in water is constant, the surface of the phytoplankton is assumed to be in equilibrium with the dissolved phase. Therefore, the flux is zero between the water and the phytoplankton surface. Then, one compartment can be taken into account for the phytoplankton phase. This approach is useful in order to simplify the derivation of an adequate equation for the air–water flux. Direct comparison between water–phytoplankton and air–water exchange is accomplished by obtaining an equation for water–phytoplankton fluxes (F_{P-W}) with the same units (ng m^{-2} d^{-1}) as air–water exchange (eq 4). This is done by first multiplying eq 1 by phytoplankton biomass (B_P) and dividing by the surface area (S_P) of the plankton cells, thus obtaining the water–phytoplankton fluxes per square meter of phytoplankton surface per day. Second, to compare these fluxes with those of air–water exchange, we must take into account all the phytoplankton cells within the mixing depth (h_{mix}, m), which is the fraction of the water column directly influenced by air–water exchange (Figure 1). Therefore, eq 1 should also be multiplied by the ratio of phytoplankton surface area to air–water surface area, which is given by the product of h_{mix} and S_P. These modifications of eq 1 give the fluxes between phytoplankton and water per square meter of water column and day, the same units as for air–water exchange (eq 4):

$$F_{P-W} = -h_{mix} S_P \frac{B_P}{S_P}\frac{dC_P}{dt} \tag{6}$$

F_{P-W} is positive when the flux is from phytoplankton to water (depuration) and is negative during uptake. Equation 6 may be rewritten as

$$F_{P-W} = h_{mix} k_u B_P \left(C_{P,M}\frac{k_d + k_G}{k_u} - C_W\right) \tag{7}$$

Equation 7 is analogous to that used in air–water exchange and may in fact also be derived using a two-layer model for the phytoplankton–water exchange. From eq 7, the mass-transfer coefficient between phytoplankton and water (k_{P-W}, m d^{-1}) is

$$k_{P-W} = h_{mix} k_u B_P \tag{8}$$

Water–Phytoplankton Fluxes for Nonconstant Water Concentration. When the POP concentration in water is not constant, the two-compartment model for phytoplankton uptake must be applied. The assumption that water and surface concentrations are always in equilibrium does not hold since it would lead to infinite instantaneous fluxes. Therefore, dynamic sorption and desorption constants are required for the first fast sorption step. Thus, the flux between water and phytoplankton for nonconstant water concentration is described as

$$F_{P-W} = h_{mix} k_{ad} B_P \left(C_{P,S}\frac{k_{des} + k_G}{k_{ad}} - C_W\right) + h_{mix} k_u B_P \left(C_{P,M}\frac{k_d + k_G}{k_u} - C_W\right) \tag{9}$$

where k_{des} (d^{-1}) and k_{ad} (m^3 kg^{-1} d^{-1}) are the desorption and adsorption rate constants, respectively. Equation 9 describes water–phytoplankton uptake as two independent processes, one between water and phytoplankton surface and the second between water and the plankton matrix. Even though we assume implicitly that both processes are in parallel, this assumption has virtually no influence on uptake dynamics and the results reported here. The surface sorption described by the first term in eq 9 is approximately 100 times faster than partitioning into the cells (*25*). This means that the mathematical treatment of the second term is equivalent to considering that the phytoplankton matrix is interacting with the surface rather than with the water phase directly, which would be the case when both processes are in series. In the present work, k_u and k_d are considered as water–matrix uptake and depuration rate constants in order to treat them mathematically in a manner similar to that reported elsewhere (*29, 30*). Furthermore, since the sorption described by the first term of eq 9 is 2 orders of magnitude faster than the sorption explained by the second term, $C_{P,S}$, will be at or near equilibrium with C_W. This hich means that eq 9 reduces to eq 7 when the POP water concentration is constant.

Phytoplankton Uptake and Depuration Constants. The uptake and depuration constants used in this study were obtained from laboratory experiments using a novel gas purging technique designed to maintain constant concentrations in the water phase in order to properly apply eqs 2 and 3 (*25*). The experiments were performed for 17 PCB congeners representing a wide range of octanol–water partition coefficients (K_{OW}) (Table 1). *Isochrisis galbana* was the phytoplankton species used in the experiments. Once the PCB concentrations between air and water reached equilibrium in the reactor, the phytoplankton stock was introduced. Samples of phytoplankton and water were taken

TABLE 1. Octanol–Water Partition Coefficients (K_{OW}) and Uptake and Depuration Constants for the Uptake Dynamics of PCBs by *Isochrisis galbana*[a]

PCB	log K_{OW}	$k_{ad} \times 10^{-4}$ ($m^3\ kg^{-1}\ d^{-1}$)	k_{des} (d^{-1})	$k_u \times 10^{-3}$ ($m^3\ kg^{-1}\ d^{-1}$)	k_d (d^{-1})
3	4.7	0.7	287.6	0.0082	0.41 ± 0.41
10	4.8	1.1	287.6	0.0097	0.43 ± 0.45
15	5.3	2.4	287.6	0.033	0.62 ± 0.33
19	5.0	2.6	287.6	0.050	0.55 ± 0.16
34	5.7	8.5	287.6	0.098	0.74 ± 0.28
52	5.8	8.3	287.6	0.40	0.89 ± 0.14
104	5.8	14.7	287.6	0.62	1.18 ± 0.36
100	6.2	11.5	287.6	2.2	1.49 ± 0.27
101	6.4	12.1	287.6	1.6	1.13 ± 0.19
97	6.3	10.6	287.6	1.4	1.08 ± 0.19
77	6.4	10.7	287.6	0.76	0.82 ± 0.12
118	6.7	11.6	287.6	1.9	0.94 ± 0.12
105	6.7	11.5	287.6	1.8	1.13 ± 0.15
126	6.9	12.1	287.6	2.3	1.25 ± 0.16
156	7.2	11.0	287.6	2.4	1.08 ± 0.02
180	7.4	8.2	287.6	1.3	0.53 ± 0.19
170	7.3	8.4	287.6	1.2	0.38 ± 0.21

[a] These constants were derived from Ko (*25*).

at 15 min, 1, 3, 8, 24, 48, 72, and 120 h. Details on the experimental methods used can be found elsewhere (*25*).

Estimations of k_d and $C_{P,eq}$ were obtained by the nonlinear regression of the C_P time series obtained for the individual congeners to eq 2. The PCB concentrations in phytoplankton obtained for the first data point (15 min) were used as an estimate of $K_{SA}C_W$. The estimated values of k_d ranged from 0.4 to 1.5 d^{-1} (Table 1). The values of k_u were estimated using eq 3 and had values ranging from 8.2 $m^3\ kg^{-1}\ h^{-1}$ for PCB congener 3 (4-chlorobiphenyl) to 2470 $m^3\ kg^{-1}\ h^{-1}$ for PCB congener 156 (2,3,3′,4,4′,5-hexachlorobiphenyl). The k_u values decreased for higher chlorinated congeners (Table 1). These values are comparable to those reported by Skoglund et al. for *Anabena* sp. (blue-green algae) and *Scenedesmus* sp. (chlorophyte) but higher than the values described for *Synedra* sp. (diatom) (*23*).

To estimate adsorption and desorption constants, we assumed that the first point obtained in the uptake dynamics (first 15 min) corresponds to 95% achievement of equilibrium between water and phytoplankton surface. The adsorption and desorption constants obtained for the PCB congeners using the uptake data obtained by Ko (*25*) are reported in Table 1. These data show that k_{ad} ranges between 7000 $m^3\ kg^{-1}\ d^{-1}$ for PCB congener 3 to 147 000 $m^3\ kg^{-1}\ d^{-1}$ for PCB congener 104 (2,2′,4,6,6′-pentachlorobiphenyl), decreasing for the even higher chlorinated PCBs. The values and trends in k_{ad} are also comparable to those reported by Skoglund (*23*). On the other hand, with the assumptions reported above, k_{des} is 288 d^{-1} for all PCB congeners.

Results and Discussion

Air–Water–Phytoplankton Exchange. (a) Constant Water Concentration. To determine if air–water exchange can support phytoplankton concentrations, a comparison of air–water and water–phytoplankton fluxes must be performed in a real-life situation of variable water concentrations. However, knowledge of the processes involved can be obtained in a simplified way by analysis of the constant concentration scenario. This is accomplished by directly comparing eqs 4 and 6 and obtaining an analogous equation for air–phytoplankton exchange:

$$F_{P-W} = \frac{k_{ol}k_{P-W}}{k_{ol} + k_{P-W}}\left(C_{P,M}\frac{k_d + k_G}{k_u} - \frac{C_A}{H'}\right) \qquad (10)$$

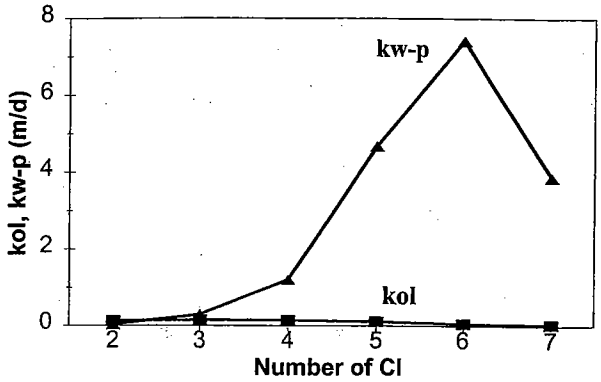

FIGURE 2. Comparison of mass-transfer rate coefficients for air–water exchange (k_{ol}) and water–phytoplankton exchange (k_{W-P}) for PCBs with a different number of chlorines. Estimation of the mass-transfer rate coefficients was done assuming a biomass of 0.3 mg/L, a mixing depth of 10 m, a wind speed of 2 m/s, and water and air temperatures of 283 K.

The limiting step will be the process with the lower mass-transfer rate. When k_{ol} and k_{P-W} are of the same order of magnitude, both air–water and water–phytoplankton exchange influence the dynamics of the air–water–phytoplankton exchange.

For example, the mass-transfer coefficients for PCBs with different numbers of chlorines (Figure 2) show that air–water–phytoplankton exchange is limited by air–water exchange for PCBs with 5–7 chlorines ($k_{ol} \ll k_{P-W}$). However, k_{ol} and k_{P-W} are of the same order of magnitude for the 2–4 Cl-substituted. This direct comparison of mass-transfer rate coefficients suggests that air–water exchange may be sufficiently fast to support phytoplankton uptake of the lower chlorinated PCBs. This contrasts with the low air–water fluxes for the higher chlorinated PCBs. Therefore in many environments, air–water exchange fluxes may be lower than the water–phytoplankton fluxes, thus leading to depleted water concentrations when other sources of pollutants are not significant. When PCB concentrations in water are constant, water–phytoplankton flux is independent of air–water exchange, and its response time is given by k_d and k_G used in eq 2.

(b) Nonconstant Water Concentration. When the water concentration of POPs is not constant, a direct comparison of k_{ol} and k_{P-W} does not indicate which mechanism is controlling the flux in the air–water–phytoplankton exchange since F_{A-W} and F_{P-W} are not the same. In this case, a dynamic simulation is performed with a known constant air concentration and low water and phytoplankton concentrations of POPs. The air concentration drives the air–water and the subsequent water–phytoplankton exchange toward equilibrium (Figure 3). The water concentration increases with time and couples the whole process of air–water–phytoplankton exchange. Water and phytoplankton concentrations of POPs increase with time and reach equilibrium long before they are equilibrated with the atmosphere.

This evaluation is complicated by the fact that there are a number of variables that must to be considered (Table 2). First of all, there are the compound-dependent physical–chemical parameters such as uptake and depuration constants, Henry's law constant (H), molecular weight, and molecular volume. There are also those variables related to environmental conditions, such as temperature, wind speed, phytoplankton biomass, phytoplankton growth rate, and mixing depth. A classical approach to study the effects of these variables would be to run the model for different values of one of the variables, keeping constant the value of all the other parameters. This procedure is time-consuming and

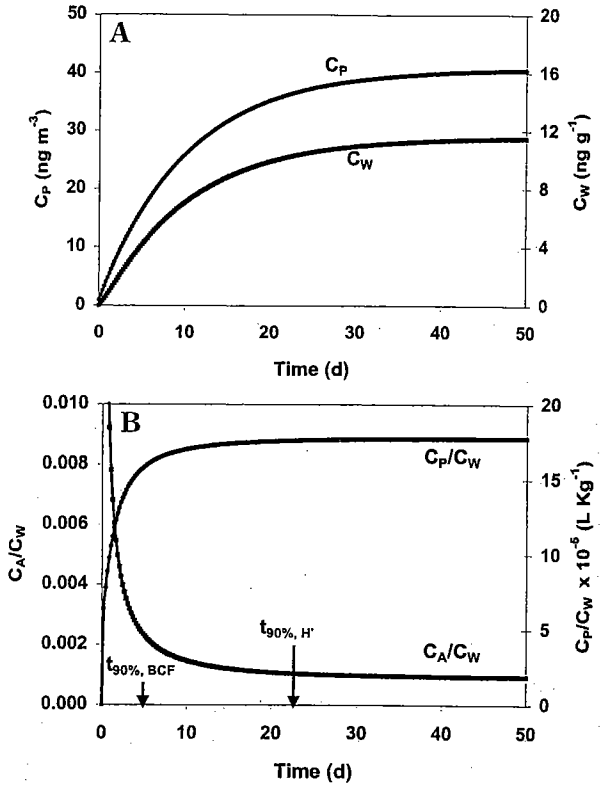

FIGURE 3. Typical example of the simulations carried out for the sensitivity analysis. The conditions used were as: $h_{mix} = 5$ m, $k_G = 0$ d^{-1}, $T = 283$ K, $U_{10} = 8$ m s^{-1}, $B_P = 0.1$ mg L^{-1}. (A) Concentrations in water (C_W) versus time; (B) Approach to equilibrium for air–water (C_A/C_W) and water–phytoplankton (C_P/C_W) during the simulation.

provides little information on the interactions between variables since they are modified one at a time. However, there are a number of statistical optimization techniques, such as simplex or experimental design approaches, that allow the effect of a large number of variables and their interactions to be studied with a minimum number of model runs. In the present paper factorial optimization, an experimental design approach, was used for the sensitivity analysis. Factorial design allows the determination of the effects of different variables and their interactions with a minimum number of runs (*31*). Interactions of three or more variables are usually negligible and/or hard to interpret; therefore a fractional factorial design was used. Details on factorial experimental design and their application to sensitivity analyses can be found elsewhere (*32, 33*).

In the present study, all the variables related to compound chemical–physical properties are considered as one variable since they cannot be modified independently. In our sensitivity analyses, this variable will be the PCB congener. In addition to different physical–chemical properties of the different PCB congeners, we accounted for wind speed, temperature, biomass, growth rate, and mixing depth. With six variables (Table 2), a full factorial design requires 64 experiments. With fractional factorial design the sensitivity analyses can be performed with 32 runs of the model. A list of the conditions for each run can be found in Table 2. The time to reach 90% of equilibrium for the air–water and water–phytoplankton exchange processes was chosen as the response time since the kinetics of both processes may be compared independently of the initial concentrations (Figure 2). Under this situation, the transfer of pollutants is from air to water and from water to phytoplankton. The time to reach 90% of equilibrium (t_{90}) is the response time of the system to changing pollutant concentrations in air. It is more convenient than to take time to 50% of equilibrium, since the latter would be dominated by the surface adsorption process and would not give an indication of the kinetics of bioaccumulation (fast + slow sorption). Response times for air–water and water–phytoplankton exchange are shown in Table 2.

The effect of each variable on the response was determined using the following equation (*32*):

$$t_{90\%} = ah_{mix} + bB_P + ck_G + dT + eU_{10} + f\text{PCB} + gh_{mix}B_P + hh_{mix}kG + ih_{mix}T + jh_{mix}U_{10} + kh_{mix}\text{PCB} + lB_Pk_G + mB_PT + nB_PU_{10} + oB_P\text{PCB} + pk_GT + qk_GU_{10} + rk_G\text{PCB} + sTU_{10} + t\text{TPCB} + uU_{10}\text{PCB} + v \quad (11)$$

where $a-v$ are the parameters obtained by fitting the response times by multiple linear regression. The t-student of these parameters allowed the determination of significance of each variable and the interactions between variables (*32, 34*). The significant variables with a confidence level higher than 95% are shown in Table 3.

Response times for water–phytoplankton exchange are dependent on phytoplankton biomass and growth rate in a complicated way since they are interacting. However, phytoplankton biomass and growth rate explain only 36% of the variability of the phytoplankton uptake response time. This is low, even though a significant correlation coefficient. The majority of the variability could not be explained due to effects of some of the variables, whose significance was not proven with the approach used, or to nonlinear effects of the variables, as assumed by the technique used in the determination of the significant variables (*32*).

No significant effect of PCB congener was observed, although the importance of uptake kinetics for the higher chlorinated PCBs has been reported (*23*). Explanations for this could be that (i) the differences in physical–chemical properties between congeners with 2 and 5 chlorines are not sufficient to provide significantly different response times or (ii) the effect of the different congener-specific physical–chemical variables may cancel each other. However, the more hydrophobic PCB congeners with 6 and 7 chlorines may have very different uptake dynamics. A second complementary sensitivity analysis was performed for PCBs with 2–7 chlorines and modifying all other variables one at a time. This allowed for the determination of interactions between PCB congeners and all the other variables. Phytoplankton–water exchange response times (90% of equilibrium) were affected only by growth rate and phytoplankton biomass (Figure 4). Longer response times were obtained for higher growth rates. However, the effect on the response time to increasing phytoplankton biomass depends on the growth rate, which led to shorter response times at constant biomass (zero growth rate) and longer response times for higher growth rates.

Higher growth rates yield longer equilibration times, since new biomass needs to reach equilibrium with the water phase. This factor increases in importance as chemical hydrophobicity increases. This is in contrast to the case of constant water concentrations where response times decreased with k_G (see eq 2). Higher phytoplankton biomass in the absence of phytoplankton growth depletes the water phase faster, achieving equilibrium somewhat faster (Figure 4). However when the phytoplankton biomass is increasing ($k_G > 0$), times to achieve equilibrium are longer (Table 3) due to the equilibration requirements of the new biomass introduced in the system.

An important result of the present study is the influence of phytoplankton uptake of POPs on the dynamics of air–water exchange. This is suggested by the effect of phytoplankton related parameters such as phytoplankton growth rate and biomass, in addition to wind speed and PCB

TABLE 2. Variable Matrix Used for the Runs of the Sensitivity Analyses of the Model and Response Times Obtained for Achieving 90% of Equilibrium for Air–Water ($t_{90,A-W}$) and Water–Phytoplankton Exchange ($t_{90,BCF}$)

	h_{mix} (m)	spm (mg/L)	k_G (d^{-1})	T (°C)	U_{10} (m/s)	PCB	$t_{90,BCF}$ (d)	$t_{90,A-W}$ (d)
1	5	0.05	0	5	8	110	5.2	23.8
2	20	0.05	0	5	2	110	10.2	30
3	5	0.5	0	5	2	110	17.4	115.8
4	20	0.5	0	5	8	110	18.2	140.2
5	5	0.05	0.02	5	2	110	6.8	300
6	20	0.05	0.02	5	8	110	7.4	300
7	5	0.5	0.02	5	8	110	6.4	300
8	20	0.5	0.02	5	2	110	6.8	300
9	5	0.05	0	20	2	110	4.8	38.8
10	20	0.05	0	20	8	110	8.8	37.0
11	5	0.5	0	20	8	110	10.2	14.4
12	20	0.5	0	20	2	110	18.2	239.4
13	5	0.05	0.02	20	8	110	4.8	9.4
14	20	0.05	0.02	20	2	110	6.8	300
15	5	0.5	0.02	20	2	110	5.8	300
16	20	0.5	0.02	20	8	110	6.6	300
17	5	0.05	0	5	8	10	0.8	9.0
18	20	0.05	0	5	2	10	24.8	153.8
19	5	0.5	0	5	2	10	6.6	38.6
20	20	0.5	0	5	8	10	7.2	37.2
21	5	0.05	0.02	5	2	10	8.0	37.8
22	20	0.05	0.02	5	8	10	8.8	36.4
23	5	0.5	0.02	5	8	10	6.6	9.2
24	20	0.5	0.02	5	2	10	9.0	200
25	5	0.05	0	20	2	10	5.4	24
26	20	0.05	0	20	8	10	6.4	17.6
27	5	0.5	0	20	8	10	4.8	4.4
28	20	0.5	0	20	2	10	25	104.2
29	5	0.05	0.02	20	8	10	5.2	4.2
30	20	0.05	0.02	20	2	10	8	108
31	5	0.5	0.02	20	2	10	6.6	25.8
32	20	0.5	0.02	20	8	10	7.6	5.2

TABLE 3. Variables and Interactions between Variables Affecting Air–Water and Water–Phytoplankton Exchange Response Times[a]

	h_{mix}	B_P	k_G	U_{10}	k_G PCB	B_P PCB	k_G B_P
air–water exchange	5.3 (39.4%)	121 (4.5%)	5133 (9.1%)	−8.8 (13.9%)	4228 (13.8%)	75 (9.8%)	
water–phytoplankton exchange		5.7 (17.2%)	108 (4.5%)				−264 (13.1%)

[a] Where h_{mix} is the mixing depth of the water column, B_P is the phytoplankton biomass, k_G is the phytoplankton growth rate, and U_{10} is the wind speed. The last three columns with two variables report the interactions between those two variables.

congener (*5*, *26*), on the response times of air–water exchange (Table 3). Longer response times are obtained for higher values of k_G and biomass. Since the effects of phytoplankton biomass and growth rate depend on the PCB congener, a detailed study of the air–water exchange response times generated with congeners with 2–7 chlorines was carried out as shown previously for the phytoplankton–water exchange. Air–water exchange response times increased for higher phytoplankton biomass (Figure 5). Furthermore, a dramatic increase of the air–water response time was observed for k_G different than zero. Indeed, phytoplankton growth rate has such a big influence on air–water exchange response times that, for PCBs with 6 and 7 chlorines, equilibrium between air and water cannot be reached whenever phytoplankton biomass is increasing (Figure 5). Phytoplankton uptake of POPs by new biomass induces a depletion of the water phase, retarding and even preventing the achievement of equilibrium between the gaseous and dissolved phases.

Other variables that affect air–water exchange response times are wind speed and mixing depth (Table 3). The higher the wind speed, the higher the air–water flux of POPs, yielding shorter response time for air–water exchange. Deeper mixing depth means greater amounts of water and phytoplankton biomass that need to be supported by air–water exchange.

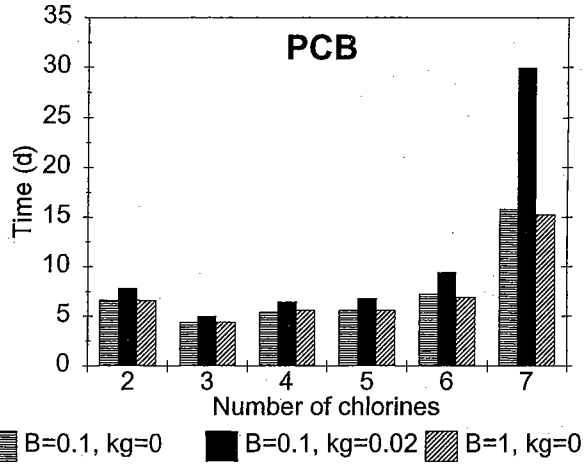

FIGURE 4. Phytoplankton–water exchange response times. Effects of growth rate and phytoplankton biomass depend on the PCB congener.

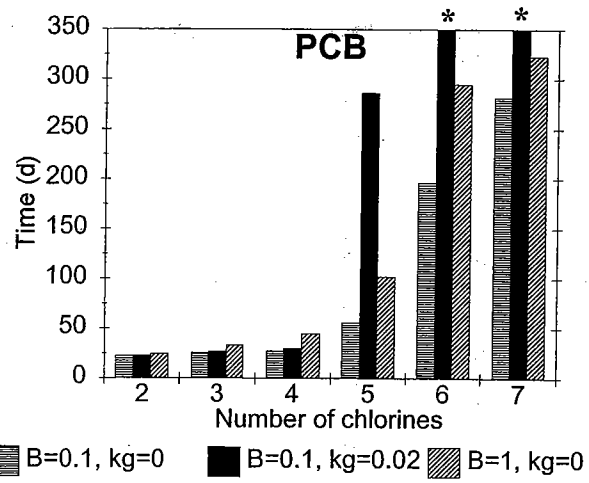

FIGURE 5. Air–water response times. Effects of phytoplankton biomass and growth rate depending on the PCB congener. An asterisk (*) means that 90% of equilibrium was never achieved during the simulations with these conditions.

Therefore, the effect of mixing depth is also linked to phytoplankton uptake.

Temperature, important in the air–water flux calculations, affects H thus modifying the equilibrium conditions between air and water. However, this study is focused on the effects on response times to reach equilibrium (a temperature-dependent state), and for this, temperature plays a secondary role. Indeed, its effect was not significant from the statistical analyses performed. The low impact of temperature on air–water exchange dynamics has been described elsewhere (*35*). Nevertheless, temperature may have an indirect effect on the air–water–phytoplankton exchange through changing biomass.

Influence of Phytoplankton Growth and Sinking on Air–Water Fluxes. Phytoplankton has an important role on the removal of PCBs from the euphotic zone by direct sinking of the phytoplankton cells or by their incorporation in zooplankton fecal pellets and subsequent sinking (*6, 7, 9, 10, 19, 36*). Even though there is controversy on whether particle export is linked to phytoplankton production in surface waters (*37, 38*), a recent review on the topic concluded that higher export rates from surface waters are related to phytoplankton productivity for blooms at high latitudes and spring blooms at mid-latitudes with food webs dominated by large phytoplankton, such as diatoms (*39*). Therefore, phytoplankton growth and the subsequent enhanced vertical export from the euphotic zone is a major sequestration process of POPs from the atmosphere, since POPs removed from the surface are no longer available for air–water exchange.

Phytoplankton uptake of POPs does not affect the magnitude of the mass-transfer coefficient between air and water (k_{ol}) since phytoplankton-related variables are not used in its estimation. However, phytoplankton uptake and the associated removal from the mixing layer to deep waters decreases the PCB concentrations in the dissolved phase, thus inducing an increase in the flux from air to water given by eq 4. Alternatively, if net volatilization dominates, then increased phytoplankton productivity and vertical sinking in the water column would lead to a decrease in the volatilization of POPs. These phenomena were directly observed in the Experimental Lakes Area (ELA) of Canada (*19*) as well as in planktonic model ecosystems (*9, 40*). This further suggests that air–water–phytoplankton exchange may be the major driving force in the biogeochemical cycles of POPs in marine and many limnetic systems.

Model Application to Lakes 227 and 110. The coupled air–water–phytoplankton model described was applied to experimental data from the remote lakes 227 and 110 in the ELA of northwestern Ontario, Canada (93°41′ W, 49°41′ N) in order to determine whether it can describe the biogeochemical cycles occurring in those lakes.

Lakes 110 and 227 have similar physical limnological characteristics, (volume, surface area, and watershed area) but differ in trophic status. Lake 110 is naturally oligotrophic but L227 has been artificially eutrophied by epilimnetic addition of phosphorus and nitrogen since 1969 (*41*). Both physical and biological processes as well as their influence on the biogeochemical cycles of PCBs and PAHs have been studied in detail and reported elsewhere (*19, 41–45*).

Mass budgets for total PCBs in lakes 110 and 227 (*19*) identify air–water exchange, atmospherically derived watershed inputs, and vertical sinking of particles as the major inputs/outputs of pollutants in these lakes. To validate the model, we calculated the mass balance for a number of PCB congeners. However, in the present paper we will focus the discussion on the results obtained for the PCB congener 52 (2,2′,5,5′-tetrachlorobiphenyl). The mass balance for this congener allowed us to determine the total input of PCB 52 from the watershed during the stratified season. Since there are no definable stream inflows, it is not possible to know the temporal variability of this watershed input. However, the only potential sources of PCB to the watershed are atmospheric deposition (dry + wet) and diffusive air–water exchange. We argue that these air–watershed fluxes are related and even proportional to the PCB air concentrations. Thus, potential runoff PCBs to the lakes follows the temporal trends of these inputs. Therefore, we assumed that the temporal variability of the watershed input was proportional to the measured atmospheric gas-phase concentration. Losses of PCBs from the photic zone due to vertical sinking of phytoplankton were estimated from vertical fluxes of particulate matter measured in the field (*45*).

The simulations were performed using measured concentrations of PCB52 in air and water (dissolved and particulate) as initial conditions. Then, the measured gas-phase concentrations of PCB52 became the driving force for incorporation into the lake biomass. Other variables needed to perform the calculations (Table 4) were biomass, sinking particulate flux, water temperature, wind speed, and mixing depth. Measured values from each system were used (*19, 45*) with linear interpolations between the sample points. Phytoplankton growth rates were estimated from biomass and sinking particulate fluxes ($F_{settling}$) by assuming that phytoplankton accounted for all the sinking material as follows:

$$k_G = \frac{1}{B_{P,t}}\left(B_{P,t+dt} - B_{P,t}\left(1 - \frac{F_{settling}}{B_{P,t}h_{mix}}\right)\right) \qquad (12)$$

where $B_{P,t}$ and $B_{P,t+dt}$ are the simulated biomass at time t and $t + dt$, respectively. Since negative values of k_G are meaningless, in case that eq 12 resulted in a negative value, a value of zero was set for k_G. Wind speed was simulated using a Weibull distribution in order to take into account the nonlinear dependence of the air–water mass-transfer coefficient with wind speed over the sampling period (*46*). PCB52 concentrations in the water and phytoplankton were predicted by the output of the model.

Figure 6 shows the comparison of the predicted PCB52 concentrations in phytoplankton, with the temporal concentrations measured on sediment trap material–phytoplankton (*19*). Phytoplankton dominated the composition of the sediment traps, with less than 10% of the mass due to zooplankton, pollen, and detritus. In these lakes, sediment traps are better surrogates for phytoplankton than the suspended particulate matter, since the latter has contribu-

TABLE 4. Values of PCB 52 Concentrations in Air, Temperature, Phytoplankton Biomass, and Total Particulate Vertical Flux Used in the Simulations for Experimental Lakes 110 and 227

		biomass (mg L^{-1})		particulate vertical flux (mg m^{-2} d^{-1})	
C_A (pg m^{-3})	temp (°C)	lake 110	lake 227	lake 110	lake 227
2.9 (Jun 2)	14 (Jun 2)	0.6 (Jun 2)	2.4 (Jun 2)	583 (Jun 2–15)	860 (Jun 2–15)
4.0 (Jun 8)	18 (Jun 14)	0.8 (Jun 14)	4.3 (Jun 15)	419 (Jun 15–28)	732 (Jun 15–28)
6.2 (Jun 14)	19 (Jul 2)	0.7 (Jun 28)	12.2 (Jun 27)	480 (Jun 28–Jul 13)	527 (Jun 28–Jul 14)
6.9 (Jun 28)	16 (Jul 16)	1.0 (Jul 12)	34.3 (Jul 12)	610 (Jul 13–26)	529 (Jul 14–28)
8.8 (Jul 6)	13 (Aug 2)	0.9 (Aug 8)	19.4 (Jul 27)	568 (Jul 26–Aug 9)	602 (Jul 28–Aug 9)
10.8 (Jul 12)	13 (Aug 17)	1.0 (Aug 22)	18.6 (Aug 10)	574 (Aug 9– Sep 9)	3050 (Aug 9–24)
8.0 (Jul 19)	15 (Sep 9)	1.6 (Sept 6)	3.7 (Aug 7)		3088 (Aug 24–Sep 7)
3.6 (Jul 26)			6.1 (Sep 7)		
5.3 (Aug 2)					
3.6 (Aug 9)					
3.4 (Aug 17)					
3.6 (Sep 4)					
7.9 (Sep 9)					

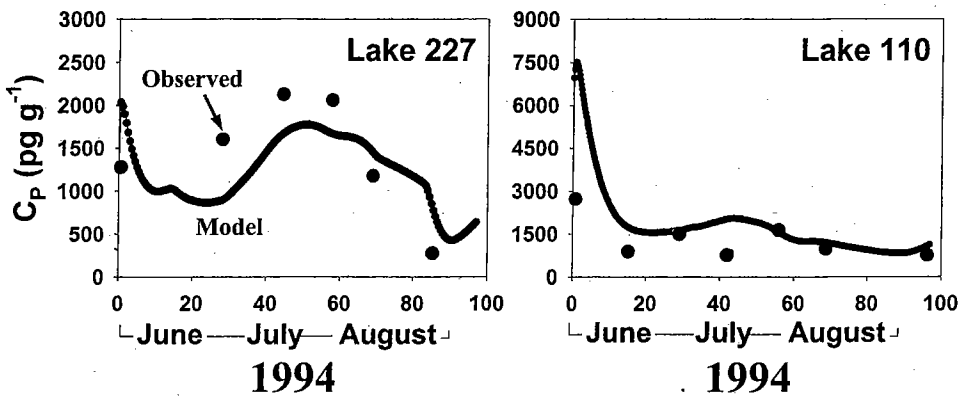

FIGURE 6. PCB congener 52 concentrations in phytoplankton. The dots are the observed concentration in phytoplankton (*19*), and the line is the trend in concentration predicted by the model.

tions from bacteria and detritus (*37*). For lake 227, the dynamic model for air–water–phytoplankton exchange predicts the observed PCB 52 concentration with an average relative difference of 25 ± 16%, where the relative difference or errors were estimated as

$$\text{error} = \left|\frac{C_{P,\text{predicted}} - C_{P,\text{observed}}}{C_{P,\text{predicted}}}\right| \times 100 \qquad (13)$$

However, equally important as the actual prediction of the concentrations is that the model accurately reflects the temporal trend of PCB52 concentrations, pointing out the importance of dynamic versus equilibrium models when modeling the environment (*35, 47*). For lake 110, the predicted and observed PCB 52 concentrations in phytoplankton showed similar relative differences (23 ± 23%). Due to transfer of pollutants from the enriched water to the phytoplankton, the model predicts a high PCB 52 concentration during the time period just after the first data point as shown in Figure 6.

Cyanobacteria were the dominant phytoplankton species in lake 227 for most of the stratified season, while lake 110 had greater phytoplankton diversity with important contributions of diatoms and chrysophyte and to a lesser extent, cryptophyte and chlorophyte. Even though the simulations for lakes 110 and 227 were performed using uptake and depuration constants for PCB accumulation in *Isochrysis galbana* (chrysophyte), an excellent fit between experimental observations and model output was obtained. This suggests that species-dependent kinetic factors may play a secondary role in the biogeochemical cycles, at least for some phytoplankton species such as cyanobacteria, chlorophytes, and chrysophytes with similar uptake and depuration coefficients (*23, 25*).

Finally, the present simulations confirm our hypothesis that air–water exchange and other atmospheric-derived inputs effectively support the POP concentrations in phytoplankton. Furthermore, this process may have a major role in the global cycling of POPs, since the world oceans are atmospherically driven. The model results also point out the relevant role of phytoplankton, which is a dominant source of organic matter in aquatic environments (*48, 35*), in removal of hydrophobic pollutants from the atmosphere by air–water exchange, and in incorporation into phytoplankton with subsequent sinking to deep waters and a fraction to sediments. Further research is needed in order to obtain a conclusive validation of the model as well as to take into account food web structure as a factor influencing air–water exchange of POPs as has been observed for carbon (*44*).

Acknowledgments

J.D. acknowledges a postdoctoral fellowship from the Spanish Ministry of Education and Culture. This work is the result of research sponsored by the United States Environmental Protection Agency (Grant EPA CR 822046-01-0, Alan Hoffman, NERL/RTP, Project Officer) and by the Minnesota Sea Grant College Program supported by the NOAA Office of Sea Grant, United States Department of Commerce, under Grant NA46-RG0101.

Literature Cited

(1) Schwarzenbach, R. P.; Gschwend, P. M.; Imboden, D. M. *Environmental Organic Chemistry*; John Wiley & Sons: New York, 1993.

(2) Achman, D.; Hornbuckle, K. C.; Eisenreich, S. J. *Environ. Sci. Technol.* **1993**, *27*, 75−86.
(3) Swackhamer, D. L.; Skoglund, R. S. *Organic Substances and Sediments in Water*, Vol. II; Baker, R., Ed.; Lewis Publishers: Boca Raton, FL, 1991; pp 91−105.
(4) Iwata, H.; Tanabe, S.; Sakal, N.; Tatsukawa, R. *Environ. Sci. Technol.* **1993**, *27*, 1080−1098.
(5) Eisenreich, S. J.; Hornbuckle, K. C.; Achman, D. R. In *Atmospheric Deposition of contaminants to the Great Lakes and Coastal Waters*; Baker, J. E., Ed.; SETAC Press: Pensacola, FL, 1997; pp 109−136.
(6) Fowler, S. W.; Knauer, G. A. *Prog. Oceanogr.* **1986**, *16*, 147−194.
(7) Baker, J. E.; Eisenreich, S. J.; Eadie, B. J. *Environ. Sci. Technol.* **1991**, *25*, 500−509.
(8) Lipiatou, E.; Mary, J.-C.; Saliot, A. *Mar. Chem.* **1993**, *44*, 43−54.
(9) Millard, E. S.; Halfon, E.; Minns, C. K.; Charlton, C. C. *Environ. Toxicol. Chem.* **1993**, *12*, 931−946.
(10) Dachs, J.; Bayona, J. M.; Fowler, S. W.; Miquel, J. C.; Albaigés, J. *Mar. Chem.* **1996**, *52*, 75−86.
(11) Broman, D.; Naf, C.; Axelman, J.; Bandh, C.; Pettersen, H.; Johnstone, R.; Wallberg, P. *Environ. Sci. Technol.* **1996**, *30*, 1238−1241.
(12) Dachs, J.; Bayona, J. M.; Raoux, C.; Albaigés, J. *Environ. Sci. Technol.* **1997**, *31*, 682−688.
(13) Dachs, J.; Bayona, J. M.; Albaigés, J. *Mar. Chem.* **1997**, *57*, 313−324.
(14) Gunnarsson, J.; Broman, D.; Jonsson, P.; Olsson, M.; Rosenber, R. *Ambio* **1995**, *24*, 383−385.
(15) Taylor, W. D.; Carey, J. H.; Lean, D. R. S.; McQueen, D. J. *Can. J. Fish. Aquat. Sci.* **1991**, *48*, 1960−1966.
(16) Richter, G.; Peters, R. H. *Environ. Toxicol. Chem.* **1993**, *12*, 207−218.
(17) Nimi, A. J.; Cho, C. Y. *Can. J. Fish Aquat. Sci.* **1981**, *38*, 1350−1356.
(18) Axelman, J.; Broman, D.; Näf, C. *Environ. Sci. Technol.* **1997**, *31*, 665−669.
(19) Jeremiason, J. D.; Eisenreich, S. J.; Paterson, M. J.; Beaty, K. G.; Hecky, R.; Elser, J. J. *Limnol. Oceanogr.* **1999**, *44*, 889−902.
(20) Gunnarsson, J.; Schaanning, M. T.; Hylland, K.; Sköld, M.; Eriksen D. Ø; Berge, J. A.; Skei, J. *Mar. Pollut. Bull.* **1996**, *33*, 80−89.
(21) Thomann, R. V.; Connolly, J. P.; Parkerton, T. F. *Environ. Toxicol. Chem* **1992**, *11*, 615−629.
(22) Skoglund, R. S.; Swackhamer, D. L. In *Environmental Chemistry of Lakes and Reservoirs*; Baker, L. A., Ed.; Advances in Chemistry Series 237; American Chemical Society: Washington, D,C, 1994; pp 559−573.
(23) Skoglund, R. S.; Stange, S.; Swackhamer, D. L. *Environ. Sci. Technol.* **1996**, *30*, 2113−2120.
(24) Ashizawa, D. J. M.S. Dissertation, State University of New York, Stony Brook, NY, 1996.
(25) Ko, F. C. Ph.D. Dissertation, University of Maryland, College Park, MD, 1994.
(26) Hornbuckle, K. C.; Jeremiason, J. D.; Sweet, C. W.; Eisenreich, S. J. *Environ. Sci. Technol.* **1994**, *28*, 1491−1501.
(27) Hornbuckle, K. C.; Sweet, C.; Pearson, R.; Swackhammer, D.; Eisenreich, S. J. *Environ. Sci. Technol.* **1995**, *29*, 869−877.
(28) Nelson E. D.; Macconnell L. L.; Baker J. E. *Environ. Sci. Technol.* **1998**, *32*, 912−919.
(29) Thomann, R. V.; Connolly, J. P. *Environ. Sci. Technol.* **1984**, *18*, 65−71.
(30) Connolly, J. P.; Pedersen, C. J. *Environ. Sci. Technol.* **1984**, *22*, 99−103.
(31) Berthouex, P. M.; Brown L. C. *Statistics for Environmental Engineers*; Lewis Publishers: Boca Raton, FL, 1994.
(32) Box, G. E. P.; Hunter W. G.; Hunter, J. S. *Statistics for Experimenters: An Introduction to Design, Data Analysis, and Model Building*; Wiley-Interscience: New York, 1978.
(33) Saltelli, A.; Andres, Th.; Homma, T. *Comput. Stat. Data Anal.* **1995**, *20*, 387−407.
(34) Dachs, J.; Fernandez, I.; Bayona, J. M. *Anal. Chim. Acta* **1997**, *351*, 377−385.
(35) Wania, F.; Haugen, J. E.; Lei, Y. D.; Mackay, D. *Environ. Sci. Technol.* **1998**, *32*, 1013−1021.
(36) Gustafsson, Ö.; Gschwend, P. M.; Buesseler, K. O. *Environ. Sci. Technol.* **1997**, *31*, 3544−3550.
(37) Valiela, I. *Marine Ecological Processes*; Springer-Verlag: New York, 1995; pp 385−424.
(38) Rivkin, R. B.; Legendre, L.; Deibel, D.; Trembay, J. E.; Klein, B.; Crocker, K.; Roy, S.; Silverberg, N.; Lovejoy, C.; Mesple, F.; Romero, N.; Anderson, M. R.; Matthews, P.; Savenkoff, C.; Vezina, A.; Therriault, J. C.; Wesson, J.; Berube, C.; Ingram, R. G. *Science* **1996**, *272*, 1163−1166.
(39) Buesseler, K. O. *Global Biogeochem. Cycles* **1998**, *12*, 297−310.
(40) Millard, E. S.; Charlton, C. C.; Burnison, G. A. *Arch. Environ. Contam. Toxicol.* **1983**, *12*, 203−210.
(41) Hecky, R. E.; Rosenberg, D. M.; Campbell, P. *Can. J. Fish Aquat. Sci.* **1994**, *51*, 2243−2246.
(42) Schindler, D. W. *Science* **1974**, *184*, 879−899.
(43) Hendzel, L. L.; Hecky, R. E.; Findlay, D. L. *Can. J. Fish Aquat. Sci.* **1994**, *51*, 2247−2253.
(44) Schindler, D. E.; Carpenter, S. R.; Cole, J. J.; Kitchell, J. F.; Pace, M. L. *Nature* **1997**, *277*, 248−251.
(45) Jeremiason, J. D. Ph.D. Dissertation, University of Minnesota, Minneapolis, 1997.
(46) Livingstone D. M.; Imboden, D. M. *Tellus* **1993**, *45B*, 275−295.
(47) Dachs, J.; Eisenreich, S. J.; Hoff, R. M. Submitted for publication in *Environ. Sci. Technol.*
(48) Duce, R. A.; Duursma, E. K. *Mar. Chem.* **1977**, *5*, 319−339.

Received for review February 12, 1999. Revised manuscript received August 12, 1999. Accepted August 13, 1999.

ES990168O